

Two-dimensional diffusion of hydrogen in  $\text{ZrBe}_2\text{H}_{1.4}$ 

A. F. McDowell, C. F. Mendelsohn, and Mark S. Conradi  
*Department of Physics-1105, Washington University, St. Louis, Missouri 63130*

R. C. Bowman, Jr.  
*Aerojet Electronic Systems, P.O. Box 296, Azusa, California 91702*

A. J. Maeland  
*Institute for Energy Technology, P.O. Box 40, N-2007, Kjeller, Norway*  
 (Received 15 July 1994; revised manuscript received 26 October 1994)

The diffusion of hydrogen through the hexagonal metal hydride  $\text{ZrBe}_2\text{H}_{1.4}$  has been studied by measuring the  $^1\text{H}$  nuclear spin-lattice relaxation rate  $T_1^{-1}$  as a function of frequency and temperature. At high temperatures, where the hopping rate of the H interstitials is faster than the nuclear magnetic resonance (NMR) frequency, the relaxation rate has a frequency dependence much larger than expected for random diffusive motion in three dimensions. A previous NMR study of  $\text{ZrBe}_2\text{H}_{1.4}$  did not account for the anomalous frequency dependence. Our data more fully define the frequency dependence, and we find that it is consistent with a model in which the motion of the hydrogen is restricted to two dimensions. Two-dimensional motion allows a self-consistent analysis of the  $T_1^{-1}$  data for all the measured frequencies and provides an improved measure of the activation energy,  $E_a = 0.27 \pm 0.02$  eV. The frequency dependence of  $T_1^{-1}$  can be used to identify two-dimensional motion in a randomly oriented powder sample.

## I. INTRODUCTION

Metal hydrides are technologically attractive materials due to their ability to store high volumetric densities of hydrogen safely and their applications in commercially viable rechargeable batteries. However, common metal hydrides are quite heavy, rendering them less optimal for applications where portability is desired. Hence, there has been interest in developing light, beryllium-based metal hydrides (pure beryllium is not suitable for hydrogen storage). Of the beryllium-containing intermetallic compounds (and one amorphous alloy) previously tested, only  $\text{ZrBe}_2$  (and the very similar  $\text{HfBe}_2$ ) showed promise as a hydrogen storage material.<sup>1</sup>

$\text{ZrBe}_2$  crystallizes with the hexagonal  $\text{AlB}_2$ -type structure. The Zr atoms lie at (0,0,0) while the two Be atoms are at  $(1/3, 1/3, 1/2)$  and  $(2/3, 2/3, 1/2)$  in the unit cell (see Fig. 1). The structure of  $\text{ZrBe}_2\text{D}_{1.5}$  has the same symmetry as  $\text{ZrBe}_2$ .<sup>2</sup> Room temperature neutron diffraction studies show that the deuterium atoms reside in the hexagonal Zr planes at the centers of triangles formed by the Zr atoms. The Be atoms lie directly above and below the D atoms in the  $c$  direction. The addition of 1.5 deuterium atoms per unit cell to  $\text{ZrBe}_2$  causes a 7.3% elongation of the  $c$  axis and a 2.7% contraction of the  $a$  axes. It is believed that this structural distortion indicates that the Zr-D attraction is much stronger than the Be-D attraction in  $\text{ZrBe}_2\text{D}_{1.5}$ .<sup>2</sup> No ordering of the site occupancy of the D atoms was observed at room temperature.

Westlake<sup>3</sup> has predicted, based on geometrical considerations, that H atoms in  $\text{ZrBe}_2\text{H}_{1.4}$  will reside in sites just above and below the Zr planes. These two sites

are separated by only 0.12 Å. Occupation of the off-plane sites has been observed for  $T < 260$  K by neutron diffraction.<sup>4</sup> The NMR relaxation rate  $T_1^{-1}$  is not sensitive to the presence of this small off-plane displacement.

The diffusion of hydrogen through the metal is crucial to all the technological applications of metal hydrides. The effective repulsion between the Be and H atoms, which gives rise to the elongation of the  $c$  axis, suggests<sup>3</sup> that the H atoms will avoid coming near the Be atoms. Since the Be atoms block direct H jumps from one Zr plane to the next, H hops may well be constrained to lie within the Zr plane. Indeed, the present work presents a demonstration of two-dimensional motion in this metal hydride. We note that two-dimensionally restricted mo-

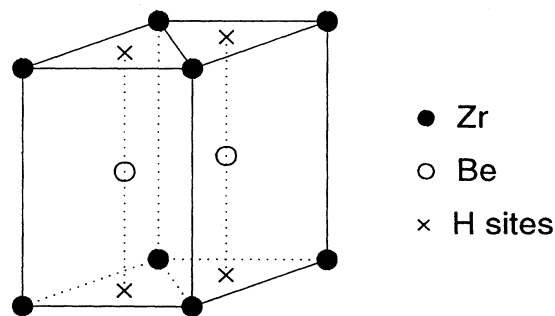


FIG. 1. The hexagonal unit cell of  $\text{ZrBe}_2\text{H}_{1.4}$ . The Zr atoms form hexagonal planes. The H sites are at the centers of triangles formed by Zr atoms. The Be atoms lie between two H sites. Full occupation of the H sites would correspond to  $\text{ZrBe}_2\text{H}_2$ .

tion has been postulated for TiCuH<sub>0.94</sub> in order to explain the difference in activation energies for H motion in this sample and in TiH<sub>2</sub>.<sup>5</sup>

In *elemental* hexagonal hydrides (e.g.,  $\alpha$ -YH<sub>x</sub>) the hydrogen motion is not two dimensional. In these materials, the hydrogen atoms occupy tetrahedral sites *between* (equivalent) planes of metal atoms. The situation is quite different in ZrBe<sub>2</sub>H<sub>1.4</sub>. The hydrogen atoms are at hexahedral sites *in* the Zr planes and are separated from adjacent planes of sites by (inequivalent) Be layers. Hence, hydrogen motion in ZrBe<sub>2</sub>H<sub>1.4</sub>, unlike motion in elemental hexagonal hydrides, is expected to be substantially anisotropic.

Measurements of the <sup>1</sup>H nuclear magnetic spin-lattice relaxation rate  $T_1^{-1}$  are often used to determine the diffusive hopping rate  $\tau_D^{-1}$  as a function of temperature.<sup>6</sup> A theory linking a model for the H motion to the relaxation rate is necessary to determine  $\tau_D^{-1}$  from  $T_1^{-1}$ . The frequency dependence of the relaxation rates due to diffusive motion in one, two, and three dimensions is well understood in certain limits,<sup>7</sup> and this frequency dependence helps identify the proper model for the H motion. When the hop rate is slow compared to the NMR frequency  $\omega_0$  ( $\omega_0\tau_D \gg 1$ ),  $T_1^{-1} \propto \omega_0^{-2}$  regardless of the dimensionality of the motion. However, in the limit of motion fast compared to the NMR frequency ( $\omega_0\tau_D \ll 1$ ), the frequency dependence of  $T_1^{-1}$  depends on the dimensionality of the motion. For isotropic three-dimensional motion, there is no frequency dependence to lowest order [that is, the spectral density  $J(\omega)$  tends to a finite limiting value as  $\omega \rightarrow 0$ ], while for motion restricted to two dimensions, there is a logarithmic dependence of  $T_1^{-1}$  on  $\omega_0$ . We have measured a frequency dependence of  $T_1^{-1}$  for a powdered sample of ZrBe<sub>2</sub>H<sub>1.4</sub> in the fast motion regime that indicates that the H motion is not isotropic in three dimensions. Instead, the frequency dependence is consistent with the model of H motion constrained to the Zr planes. We note that NMR allows the determination of the dimensionality of the motion without requiring orientable single crystal samples.

A previous NMR study of ZrBe<sub>2</sub>H<sub>1.4</sub>,<sup>8</sup> which focused on the behavior of  $T_1^{-1}$  when  $\omega_0\tau_D \geq 1$ , determined an activation energy of  $0.18 \pm 0.02$  eV. However, the analysis leading to this value could explain the frequency dependence of  $T_1^{-1}$  only by including an unphysical frequency dependence (or, equivalently, field dependence) in  $\tau_D^{-1}$ . By accounting for the two-dimensional nature of the motion, the analysis of our  $T_1^{-1}$  data provides an internally consistent description of the hydrogen motion and an activation energy of  $E_a = 0.27 \pm 0.02$  eV.

## II. EXPERIMENTAL DETAILS

The preparation procedures for the powdered samples have been reported previously.<sup>1</sup> Measurements were made in magnetic fields up to 2 T in a Varian XL-100 electromagnet fitted with a NMR field stabilizer. <sup>1</sup>H nuclear spin relaxation rates were measured using a computer-controlled pulsed NMR spectrometer. The resonance line was never more than 2 kHz wide [full width

at half maximum (FWHM)] and so always fell entirely within the bandwidth of the radiofrequency pulses.  $T_1$  was measured using an inversion-recovery technique and fitting the integrated free induction decay as a function of recovery time  $t$ :

$$M(t) = M(\infty)[1 - A \exp(-t/T_1)] .$$

The parameter  $A$  was typically 1.95, indicating nearly full inversion. The recovery curves were exponential over at least two orders of magnitude.

The spin-spin relaxation rate  $T_2^{-1}$  (the rate of irreversible dephasing) was measured using a simple spin-echo sequence,  $\pi/2$ - $\tau$ - $\pi$ - $\tau$ -echo, as well as the Carr-Purcell-Meiboom-Gill<sup>9,10</sup> (CPMG) sequence  $\pi/2$ - $\tau$ - $(\pi$ - $\tau$ -echo- $\tau)^n$ . In both cases, some of the echo amplitude versus time plots were not exponential, and in these circumstances we defined  $T_2$  as the  $1/e$  point on the decay curve.

The applied magnetic fields were chosen to reproduce the resonance frequencies of the previous NMR work on ZrBe<sub>2</sub>H<sub>1.4</sub>.<sup>8</sup> Our data extend the previous data to temperatures high enough to fully demonstrate the high-temperature frequency dependence of  $T_1^{-1}$ . Our data at 34.5 MHz agree exactly with the earlier work, while for the other frequencies our relaxation rates deviate systematically toward lower values for temperatures below 275 K. In our experiments, temperatures were varied and controlled by thermostatted flowing gas. The temperatures were steady to within  $\pm 1$  K and were measured with a copper-Constantan thermocouple placed within 0.5 cm of the sample. In light of the discrepancy with the previous work, we have been careful to check that the temperature measurements were independent of detailed placement of the thermocouple and that the NMR results did not depend on the thermal history of the experiment. In the previous work, the 34.5 MHz data were taken on a different spectrometer/magnet system than the other frequencies. It has been suggested<sup>11</sup> that the discrepancy between our results and the previous publication reflects errors in thermometry in the earlier measurements. We believe our temperatures are more accurate.

We note that our  $T_1^{-1}$  data at 34.5 MHz agreed with the previous work to within  $< \pm 5\%$  over the entire temperature range. Hence, in our plots of  $T_1^{-1}$  vs  $10^3/T$ , the uncertainty in  $T_1^{-1}$  is comparable to the size of the symbols. This is also visible in the scatter of our data about the smooth curves expected for relaxation rate peaks.

## III. EXPERIMENTAL RESULTS AND DISCUSSION

Figure 2 shows the relaxation rates  $T_1^{-1}$  as a function of temperature, measured at four resonance frequencies  $\omega_0/2\pi$ . The relaxation in the temperature range shown is due to two mechanisms: interaction with conduction electron spins and modulation, due to diffusive motion, of the hydrogen magnetic dipole-dipole interactions.<sup>8</sup> Since we are interested in studying the H motion, we subtract the contribution of the conduction electrons to  $T_1^{-1}$ . The

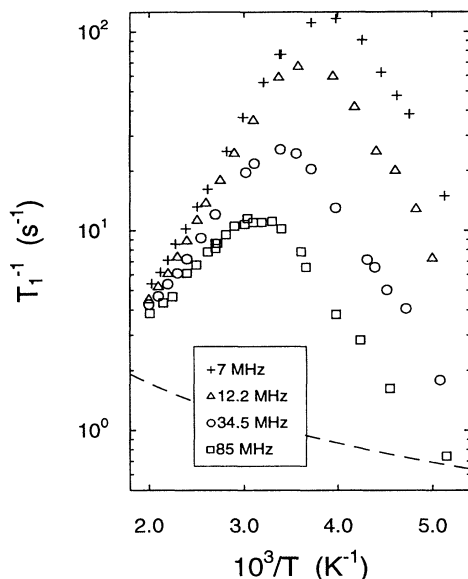


FIG. 2. The measured spin-lattice relaxation rates  $T_1^{-1}$  determined at four resonance frequencies. The rate maxima correspond to  $\omega_0\tau_c \approx 1$ . Note the nonvanishing frequency dependence at temperatures above the maxima. The dashed curve shows the relaxation contribution from conduction electron spins; the remainder of the relaxation is due to H motion. The uncertainty in  $T_1^{-1}$  is comparable to the size of the symbols.

conduction electron relaxation has a simple temperature dependence:<sup>12</sup>

$$T_{1e}T = \kappa \quad (1)$$

where  $T_{1e}$  is the relaxation time due to interaction with conduction electrons and  $\kappa$  is a sample-dependent constant. Bowman *et al.*<sup>8</sup> found  $\kappa = 290$  sK by measuring  $T_1$  at low temperatures ( $T < 150$  K) where H motion is too slow to affect the relaxation and (presumably) all of the relaxation is due to interaction with conduction electron spins. We use this value of  $\kappa$  to calculate  $T_{1e}^{-1}$  and then determine the diffusional contribution to the relaxation,  $T_{1d}^{-1}$ :

$$T_{1d}^{-1} = T_1^{-1} - T_{1e}^{-1} \quad (2)$$

$T_1^{-1}$  in this equation is the measured value, shown in Fig. 2. The values of  $T_{1d}^{-1}$  calculated using Eq. (2) are shown as a function of reciprocal temperature in Fig. 3. The size of the  $T_{1e}^{-1}$  correction is shown by the dashed curve in Fig. 2.

Figure 3 has some unusual features. At temperatures above the temperature of the relaxation rate peaks, the data retain a significant and unexpected frequency dependence. Normally, one expects that  $T_{1d}^{-1}$  data from a crystalline system such as this will be well described by the theory of Bloembergen, Purcell, and Pound (BPP),<sup>13</sup> in which a single correlation time is used to describe the motion of the hydrogen atoms and the correlation functions for the stochastic motion have exponential forms.

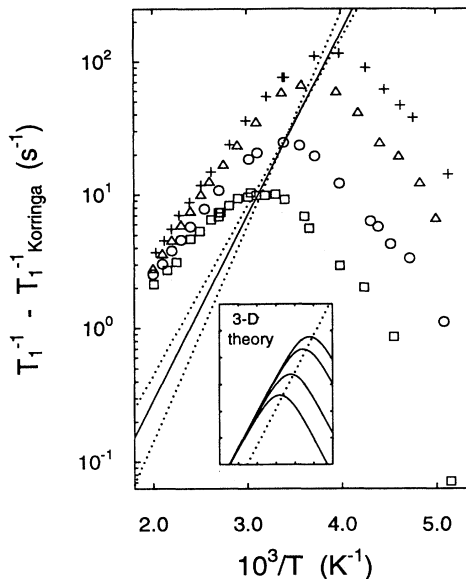


FIG. 3. The  $T_1^{-1}$  data corrected for the contribution of the conduction electron spins, at the same four frequencies as in Fig. 2. The solid line drawn through the rate peaks corresponds to  $\tau_{c0} = 9 \times 10^{-14}$  s and  $E_a = 0.27$  eV. The dotted lines show the range of acceptable lines through the peaks. The inset shows the three-dimensional (3D) theory prediction for the same four frequencies. The dotted line on the inset passes through the theoretical relaxation peaks.

Under these assumptions the relaxation rate is proportional to  $\tau_c/[1 + (\omega_0\tau_c)^2]$ , where  $\tau_c$  is the correlation time.<sup>14</sup> An estimate which includes only nearest neighbors shows that the contribution of the Be nuclei to the local magnetic field at the H site is roughly half the size of the contribution from other H atoms in the plane. There is little average contribution from the Zr nuclei due to the low abundance of <sup>91</sup>Zr. H motion modulates the H-Be interaction with  $\tau_c = \tau_D$ . H motion modulates the H-H interactions with  $\tau_c = 0.5\tau_D$ , since either spin in an interacting pair can move. The relaxation rate is expected to be independent of frequency when  $\omega_0\tau_c \ll 1$ , i.e., when the temperature is above the  $T_{1d}^{-1}$  peak. More recent Monte Carlo-based theories of relaxation in 3D systems give relaxation rate peaks that differ slightly from the BPP-predicted peaks;<sup>15</sup> these differences do not affect the present discussion. The inset in Fig. 3 demonstrates the Monte Carlo-based prediction (for 3D motion) for  $\log_{10}(T_1^{-1})$  vs  $10^3/T$  for the four frequencies of the data. Our  $T_{1d}^{-1}$  data clearly do not follow the 3D prediction, retaining a noticeable frequency dependence at temperatures above the peaks.

The BPP theory also predicts that the relaxation rate is proportional to  $\tau_c$  at temperatures above the relaxation peak ( $\omega_0\tau_c \ll 1$ ). If one assumes that the H diffusion is activated,

$$\tau_c = \tau_{c0} \exp(E_a/k_B T) \quad (3)$$

then the slope in the high-temperature region of Fig. 3 should give the activation energy  $E_a$ . (The high- and

low-temperature limiting slopes of the data in Fig. 3 all agree to within 10%.) In addition, the BPP theory predicts that the relaxation rate peak should occur when  $\omega_0\tau_c \approx 1$ . Since the peak values of  $T_1^{-1}$  in Fig. 3 are proportional to  $1/\omega_0$  (see below), the condition  $\omega_0\tau_c \approx 1$  implies that the slope of the line drawn through the peaks in Fig. 3 should also yield the same activation energy. For the BPP theory (and other 3D theories), this is indeed the case, as shown in the inset. But it is clear from Fig. 3 that the line through the *data* peaks does not have the same slope as the  $T_{1d}^{-1}$  data in the high-temperature region. The fact that these two slopes differ, a direct consequence of the frequency dependence in the high-temperature region, means that it is impossible to use the BPP theory (with a single temperature-dependent  $\tau_c$ ) to simultaneously explain all four sets of  $T_{1d}^{-1}$  data.

The positions of the  $T_{1d}^{-1}$  peaks as a function of  $1/T$  provide a relatively theory-independent determination of the activation energy. In many physical systems the correlation function has a *shape* independent of temperature, but with a temperature-dependent time scale. That is, the correlation function at all temperatures is the same, after suitable adjustment of the time scale. In these cases, the  $T_{1d}^{-1}$  peak will occur at a fixed numerical value of  $\omega_0\tau_c$ , of order 1. Furthermore, the maximum rate  $T_{1d}^{-1}$  is predicted to vary as  $\omega_0^{-1}$ . The BPP theory is an example, but many non-BPP systems are also so described.<sup>15</sup> The key condition is that there must be a single characteristic time describing the dynamics; thus essentially all crystalline systems obey this scaling.

For the above reasons, the line drawn through the  $T_{1d}^{-1}$  peaks in Fig. 3 can be used to determine  $\tau_D(T)$ . By choosing  $\omega_0\tau_c = 1$  at the peak, we find that  $\tau_{c0} = 9 \times 10^{-14}$  s and  $E_a = 0.27$  eV. A range of parameters yields lines that pass satisfactorily (as assessed by eye) through the broad peaks in Fig. 3: roughly,  $E_a = 0.25$  eV,  $\tau_{c0} = 2.5 \times 10^{-13}$  s to  $E_a = 0.32$  eV,  $\tau_{c0} = 1.6 \times 10^{-14}$  s, as indicated in Fig. 3. These  $\tau_{c0}$  values are of the expected order of magnitude, namely, the inverse of a phonon frequency,  $\omega_{ph} \approx 10^{13}$  s<sup>-1</sup>.

The measured relaxation rate  $T_{1d}^{-1}$  in Fig. 3 does obey  $(T_{1d}^{-1})_{\max} \propto (\omega_0)^{-1}$ . In *amorphous* metal hydrides, one also finds that  $(T_{1d}^{-1})_{\max} \propto (\omega_0)^{-1}$ , while the slopes of the high-temperature  $\log_{10}(T_{1d}^{-1})$  vs  $10^3/T$  data are not consistent with the slope of the line drawn through the peaks.<sup>16</sup> For amorphous samples, the unequal slopes arise from a distribution of activation energies present in the material due to static disorder. There is no evidence for such disorder in  $\text{ZrBe}_2\text{H}_{1.4}$  from the neutron diffraction experiment.<sup>2</sup> In this crystalline hydride, the anomalous frequency dependence and the corresponding breakdown of the (3D) BPP model can be explained by assuming that the diffusive hydrogen motion is constrained to two dimensions, as discussed below. The correlation functions for motion in two dimensions differ significantly from the exponentials that form the basis of the BPP theory; in particular, the correlation functions have long-time tails that decay as power laws,  $t^{-n}$ , not as exponentials. We note the  $T_{1d}^{-1}$  data in Fig. 3 at low temperatures ( $\omega_0\tau_c \gg 1$ ) are consistent with  $T_{1d}^{-1} \propto \omega_0^{-2}$ , as expected.

Figure 4 shows evidence that the hydrogen motion in  $\text{ZrBe}_2\text{H}_{1.4}$  is indeed long range. The two-pulse ( $\pi/2$ - $\tau$ - $\pi$ - $\tau$ -echo)  $T_2^{-1}$  data are independent of resonance frequency at low temperatures. As the temperature is increased and the H atoms move faster (and farther in a given time), the  $T_2^{-1}$  values deviate from the line defined by the lower-temperature data. The temperature at which this deviation occurs rises as the resonance frequency is lowered. The deviation is due to long-range H atom diffusion in the presence of a magnetic field gradient. The CPMG pulse sequence<sup>9,10</sup> partially compensates for the effects of diffusion in a field gradient, and hence the CPMG  $T_2^{-1}$  data show less deviation in Fig. 4.

For a linear field gradient,  $G = dB_z/dz$ , the echo decay curve for the two-pulse  $T_2$  experiment is given by:<sup>17</sup>

$$M(2\tau) = M_0 \exp \left[ -\frac{2\tau}{T_2} - \gamma^2 G^2 D \frac{(2\tau)^3}{12} \right] . \quad (4)$$

The magnetic field gradients in our sample arise because the sample is powdered (to permit radiofrequency field penetration). Since  $\text{ZrBe}_2\text{H}_{1.4}$  has a nonzero magnetic susceptibility  $\chi$ , each nonsymmetric powder particle creates its own inhomogeneous internal magnetic field and contributes to the field at its neighboring particles. The rms gradient will scale as the inverse of the mean particle size  $\Delta x$  and will be linear in the applied field,  $H_0$ :  $G = \Delta H/\Delta x \propto H_0\chi/\Delta x$ . Thus the frequency dependence in Fig. 4 is more fundamentally a dependence on the applied magnetic field. In the region where the  $T_2^{-1}$  values do not depend on applied field, the spin-echo decay curves are observed to be exponential, reflecting the

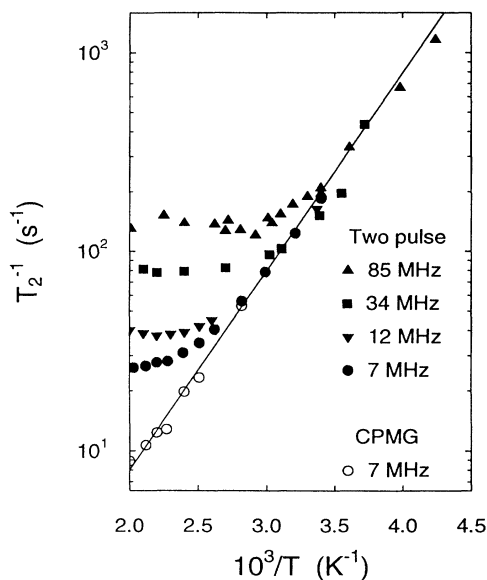


FIG. 4. The  $T_2^{-1}$  data, from spin echoes. The solid symbols are from the two-pulse experiment and the open symbols from CPMG. The plateaus in the two-pulse data are due to diffusion in the field gradients that arise from the susceptibility of the metal particles. The line is an eye guide drawn through the low-temperature data.

fact that diffusion in the field gradients has a negligible effect.  $T_2^{-1}$  is large enough and  $D$  is small enough that the first term in Eq. (4) dominates. In the region of field dependence, the decay curves have a slight curvature, corresponding to the  $(2\tau)^3$  term in the decay. We do not observe a well-defined cubic dependence on  $2\tau$ ; the sample does not consist of uniformly shaped particles and so a distribution of  $G$  values is present. The distribution of  $G$  values leads to a nearly linear decay curve with a  $1/e$  point (our definition of  $T_2$  in this case) that is almost temperature independent (see the plateaus in Fig. 4). As the applied field is increased, the plateau values of  $T_2^{-1}$  are larger because the field gradients are larger.

*Effects of dimensionality.* Spin relaxation is governed by  $G(t)$ , the two-spin relative position correlation function describing the fluctuating spin-spin interactions.<sup>13,17</sup> The relaxation rate  $T_{1d}^{-1}$  is proportional to  $J(\omega_0)$ ,<sup>13,14</sup> where  $J(\omega)$  is the Fourier transform of  $G(t)$ . The following simple but general argument can be made for the effects of dimensionality on the shape of  $G(t)$  for a *short-range, isotropic* interaction. For times not too much larger than  $\tau_D$ , the correlation function decays approximately exponentially in time. In crude terms, the exponential decay reflects the probability that either of the (neighboring) interacting spins has jumped at least once, since one jump is enough to decorrelate the spin interactions. At long times, there is a finite probability that the two spins (H and metal, or two H spins) will have *returned* to each other's proximity. From simple random-walk theory on a  $d = 1, 2,$  or  $3$  square/cubic lattice of unit length, the rms distance from the origin is  $r = N^{1/2}$  after  $N$  steps, where  $N = t/\tau_D$ . The number of lattice sites within an interval/circle/sphere of this radius is proportional to  $r^d$ , or  $N^{d/2}$ . Thus the probability of a spin being at any one site in this volume, in particular back at the origin, is proportional to  $N^{-d/2}$ . Hence, the long-time tail of the correlation function  $G(t)$  decays as  $t^{-1/2}$ ,  $t^{-1}$ , and  $t^{-3/2}$  for  $d = 1, 2,$  and  $3$ . The long-time tail also appears for the dipole-dipole interaction<sup>7</sup> (neither short ranged nor isotropic); only the amplitude of the tail is sensitive to the details of the model.

The frequency dependence of  $T_{1d}^{-1}$  in the high-temperature region ( $\omega_0\tau_c \ll 1$ ) has been shown to be<sup>7,18</sup>

$$\begin{aligned} T_{1d}^{-1} &= A\tau_D - B, \tau_D^{3/2} \omega_0^{1/2} && \text{in 3D,} \\ T_{1d}^{-1} &= C, \tau_D \ln(\omega_0/\omega_*) && \text{in 2D,} \\ T_{1d}^{-1} &= E, \tau_D^{1/2} \omega_0^{-1/2} && \text{in 1D.} \end{aligned} \quad (5)$$

( $\omega_*$  accounts for the choice of units for  $\omega_0$ ). The  $\omega_0^{1/2}$  dependence for 3D motion has been confirmed experimentally.<sup>19</sup> The  $\ln(\omega_0)$  dependence for 2D motion has been observed in graphite intercalation compounds<sup>18</sup> and other patently 2D systems.<sup>20,21</sup> The proportionality constants  $A$  and  $B$  in the equation for three-dimensional motion can be calculated for a particular model of hopping motion on a given network of atomic sites.<sup>7</sup> The proportionality constant  $C$  for a single two-dimensional plane of spins can also be calculated, using mean-field

theory.<sup>22</sup> The constant  $E$  for the one-dimensional equation is not known. It is not known how quickly the asymptotic limits given by Eq. (5) are approached.

The 2D result in Eq. (5) is for a single isolated plane of spins. The general argument given above shows that the inclusion of spin-spin interactions with off-plane spins (either the Be atoms or the neighboring H planes) cannot change the existence of a logarithmic dependence of  $T_1^{-1}$  on  $\omega_0$  in the limit  $\omega_0\tau_c \ll 1$ . However, the relative sizes of the BPP-like peak and the logarithmic variation will be affected.

Equation (5) gives the frequency dependence for rigorously 1D, 2D, or 3D motion. In a real material, motion may be anisotropic, yet not strictly 2D. There are no theoretical predictions for the shapes of the  $T_{1d}^{-1}$  maxima for this intermediate case, although one expects that as the motion becomes more isotropic there will be a smooth transition between the  $\omega_0$  dependences in Eq. (5). Qualitatively, if interplanar (IP) jumps occur at a rate  $\tau_{IP}^{-1} \ll \tau_D^{-1}$ , the 2D frequency dependence should apply for frequencies  $\omega_0$  such that  $\tau_{IP}^{-1} \ll \omega_0 \ll \tau_D^{-1}$ . Although we will find that our data are consistent with 2D hydrogen motion, relatively infrequent interplanar jumps cannot be ruled out.

We proceed by assuming our data for  $10^3/T < 2.7$  lie in the asymptotic regime and attempting to fit the frequency dependence of Fig. 3 with each of the limiting forms, Eq. (5). Unfortunately, it is not possible to span a wide frequency range while remaining in the high-temperature regime without heating the sample to excessive temperatures. As a consequence, the frequency dependence of our data does not definitively identify the dimensionality. However, the dependence of Eq. (5) on the mean residence time  $\tau_D$  can be exploited to identify the motion of hydrogen in  $ZrBe_2H_{1.4}$  as being *two-dimensional*.

In Fig. 5,  $T_{1d}^{-1}$  is plotted versus  $(\omega_0/2\pi)^{-1/2}$ ,  $\ln(\omega_0/2\pi)$ , and  $(\omega_0/2\pi)^{1/2}$ , appropriate for one-,

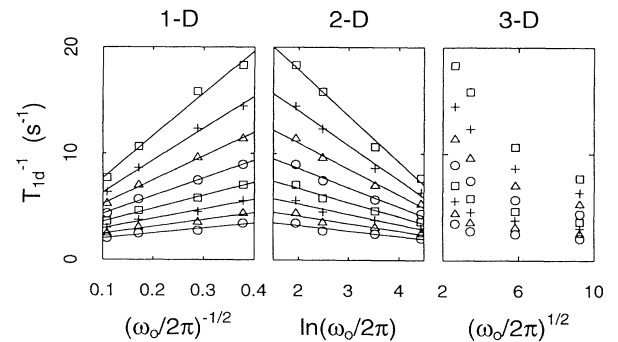


FIG. 5. Fits to the high-temperature frequency dependence of  $T_{1d}^{-1}$ , using models for one-, two-, and three-dimensional motion. The frequencies are measured in units of MHz. In each panel, the data correspond to  $10^3/T = 2.7, 2.6, \dots, 2.0$ , from top to bottom; all of these temperatures are above the  $T_{1d}^{-1}$  maxima in Fig. 3. The lines are least-squares best-fit lines. The uncertainty in the  $T_{1d}^{-1}$  values is comparable to the symbol size.

two-, and three-dimensional motion, respectively. Data are shown at temperatures such that  $10^3/T = 2.0, 2.1, \dots, 2.7$ . Linear fits to Fig. 3 were used to interpolate  $T_{1d}^{-1}$  at these temperatures. The data for a given temperature should fall on a straight line when plotted for the correct dimensionality. The lines shown in Fig. 5 are least-squares best-fit lines. The three-dimensional plot shows a large systematic deviation from linear behavior, indicating that the frequency dependence of the  $T_{1d}^{-1}$  data is inconsistent with a model of isotropic three-dimensional hydrogen motion. Furthermore, in comparison with lattice-specific three-dimensional calculations,<sup>15</sup> the magnitude of the fractional variation in the measured  $T_1^{-1}$  with frequency is much too large (see the inset of Fig. 3). The two- and one-dimensional plots are more linear. However, the scatter of the data and the narrow frequency range do not allow the determination of the dimensionality of the hydrogen motion directly from Fig. 5; both the 1D and 2D analyses fit straight lines in Fig. 5.

Equation (5) shows that the slopes of the lines drawn in Fig. 5 are related to the mean residence time  $\tau_D$ . For the one- and two-dimensional plots in Fig. 5, we have determined  $\tau_D$  [multiplied by the constants  $C$  and  $E^2$ —see Eq. (5)] as a function of  $10^3/T$ . We plot  $\log_{10}(\tau_D)$  vs  $10^3/T$  in Fig. 6.

Both the two- and one-dimensional plots in Fig. 6 show simple activated behavior for  $\tau_D$ . However, only the two-dimensional plot yields an activation energy in agreement with the value determined by the positions of the peaks in

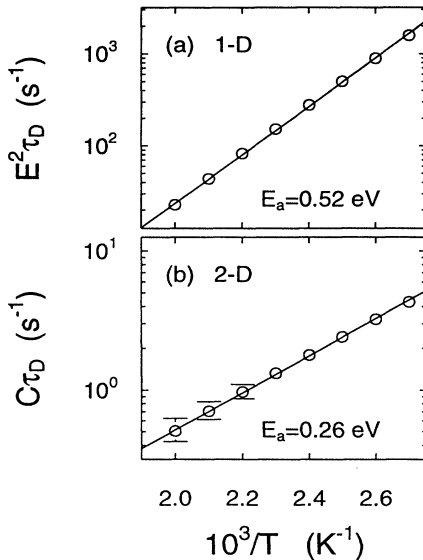


FIG. 6.  $\tau_D$  (in arbitrary units) vs  $10^3/T$  for the 1D and 2D models. The constants  $C$  and  $E$  are defined in Eq. (5). The points plotted are from the slopes in the corresponding panels of Fig. 5. The error bars indicate estimates of the errors in determining these slopes. When error bars are not explicitly shown, they are smaller than the symbols. The lines correspond to the activation energies indicated. Note the agreement of the activation energy of the 2D fit with the slope of the solid line in Fig. 3 passing through the relaxation rate peaks.

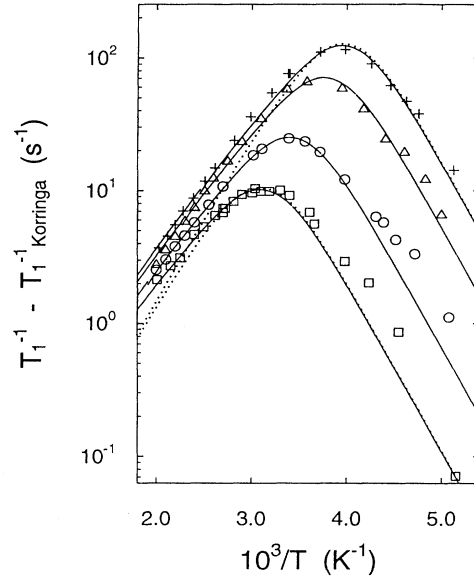


FIG. 7. Fit of the mean-field prediction for  $T_{1d}^{-1}$  of a 2D system to the data. Spherically averaged spectral densities appropriate for a single plane of square lattice (Ref. 22) were multiplied by 0.7 to generate the curves shown. The motional parameters are  $\tau_{c0} = 4 \times 10^{-14}$  s and  $E_a = 0.27$  eV. The dotted lines give the 3D theoretical prediction (using the same motional parameters) for the highest and lowest experimental frequencies.

Fig. 3. Hence, by assuming two-dimensionally restricted motion for the hydrogen atoms in  $\text{ZrBe}_2\text{H}_{1.4}$ , one can self-consistently explain the peak positions (Fig. 3) and the frequency dependence of  $T_{1d}^{-1}$  in the high-temperature region (Fig. 5), taking  $\tau_{c0} = 9 \times 10^{-14}$  s and  $E_a = 0.27$  eV.

A simultaneous fit to all the data points in Fig. 3 would be convincing proof that our two-dimensional model with an activated H hopping rate is correct. We have used the mean-field results for the spectral densities for two-dimensionally restricted motion<sup>22</sup> to make such a fit, which is shown in Fig. 7. We have used the spherically averaged results for a single square lattice of spins to calculate the curves in Fig. 7. Hence we have not included the contribution of Be-H interactions, nor the interplanar H-H interactions, to  $T_{1d}^{-1}$ . The H sites in  $\text{ZrBe}_2\text{H}_{1.4}$  form a honeycomb “lattice,” not a square lattice. We find that the calculated values of  $T_{1d}^{-1}$  must be multiplied by 0.7 in order to reproduce the maxima of the data.

Figure 7 shows that the 2D theory is very successful in explaining the high-temperature half of the relaxation rate peaks. A precise determination of the activation energy is difficult because the shapes of the theoretical curves do not match the data exactly. The optimal  $E_a$  depends whether one emphasizes the quality of fit in the high- or low-temperature region. We emphasize the high-temperature region. The curves shown in Fig. 7 correspond to  $E_a = 0.27$  eV and  $\tau_{c0} = 4 \times 10^{-14}$  s. The values  $E_a = 0.25$  eV or  $E_a = 0.29$  eV yield visibly worse fits, by eye. Although there are small systematic deviations between the 2D model and the data, the good fit clearly

demonstrates that the 2D model explains the temperature and frequency dependence of  $T_{1d}^{-1}$ , using a *single* frequency-independent, temperature-dependent correlation time  $\tau_c$ . The 3D model, as shown in Fig. 7, cannot explain the data using a single, temperature-dependent  $\tau_c$ .

In the high-temperature region, the frequency dependence of the data is slightly weaker than the frequency dependence of the 2D theory. The most obvious possible source for this is infrequent interplanar hops that introduce a small amount of 3D character into the motion. A more subtle source for the weaker frequency dependence is the relaxation due to interactions between H spins and “off-plane” spins, either Be nuclei or H spins on another Zr plane. These interactions do not share the  $\ln \omega_0$  divergence of Eq. (5), *even when H motion is strictly 2D*.<sup>22</sup> The off-plane spin interactions (expected to be weaker than in-plane interactions) introduce apparent 3D character to the relaxation, weakening the observed frequency dependence. Hence the observed deviation of the data from the 2D theory does not necessarily imply interplanar motion. We note that the 2D theory is not expected to be *exact*; it is a spherically averaged mean-field result for a square lattice. Further theoretical work, perhaps Monte Carlo simulation of H motion in the appropriate structure, could distinguish whether the weak  $\omega_0$  dependence arises from interplanar *hops* or interplanar spin *interactions*.

The data and theory also differ on the low-temperature sides of the rate peaks in Fig. 7, perhaps indicating a breakdown in the applicability of the mean-field theory in this limit: the hydrogen concentration in our sample is high,  $c = 1.4/2.0 = 0.7$ . Another possible explanation for the discrepancy is that the square lattice theory does not accurately predict the correlation function for slow motion on the honeycomb “lattice” of  $\text{ZrBe}_2\text{H}_{1.4}$ . (We find that the use of scaling factors designed to adjust the square lattice results for application to the honeycomb lattice<sup>23</sup> does not improve the fit.) Yet another possibility is that cross relaxation to the metal nuclei

occurs at lower temperatures, augmenting the relaxation rate.<sup>8</sup> Cross relaxation was observed at low temperatures ( $10^3/T > 5.0$ ) in a previous study<sup>8</sup> and may contribute to the distortion of our  $T_{1d}^{-1}$  peaks, especially at the lowest temperatures. Cross relaxation would be ineffective at higher temperatures, where the H motion is fast.

From a visual fit of the 2D theory to the  $T_{1d}^{-1}$  in Fig. 7, we find  $E_a = 0.27 \pm 0.02$  eV. The value and uncertainty of this result encompass the measurements of  $E_a$  from the peak positions (0.27 eV) and the frequency dependence (0.26 eV).

#### IV. CONCLUSIONS

Measurements of the spin-lattice relaxation rate  $T_1^{-1}$  for  $^1\text{H}$  in a powdered sample of  $\text{ZrBe}_2\text{H}_{1.4}$  have been made. The temperature and frequency dependences of the diffusional contribution to the relaxation,  $T_{1d}^{-1}$ , indicate that the motion of hydrogen is highly two dimensional.  $T_2^{-1}$  measurements demonstrate that the hydrogen motion is long ranged. The two-dimensional motion is consistent with the siting of the hydrogen atoms in the Zr planes of the hexagonal  $\text{ZrBe}_2$  host lattice. A simple application of the mean-field results for relaxation in a two-dimensional system shows that it is possible to describe both the frequency dependence of the high-temperature  $T_{1d}^{-1}$  data and the positions of the  $T_{1d}^{-1}$  maxima using a single set of hydrogen motion parameters:  $\tau_{c0} = 4 \times 10^{-14}$  s and  $E_a = 0.27 \pm 0.02$  eV.

#### ACKNOWLEDGMENTS

This work was supported by NSF Grants DMR 90-24502 and 94-03667. A.F.M. and C.F.M. gratefully acknowledge the support of the Pew Midstates Science and Mathematics Consortium, funded by a grant from the Pew Charitable Trusts.

<sup>1</sup> A. J. Maeland and G. G. Libowitz, *J. Less-Common Metals* **89**, 197 (1983).  
<sup>2</sup> A. F. Andresen, K. Ontes, and A. J. Maeland, *J. Less-Common Metals* **89**, 201 (1983).  
<sup>3</sup> D. G. Westlake, *Mater. Res. Bull.* **18**, 1409 (1983).  
<sup>4</sup> A. J. Maeland (unpublished).  
<sup>5</sup> R. C. Bowman, Jr., A. Attalla, and A. J. Maeland, *Solid State Commun.* **27**, 501 (1978).  
<sup>6</sup> R. M. Cotts, in *Electronic Structure and Properties of Hydrogen in Metals*, edited by P. Jena and C. B. Satterthwaite (Plenum, New York, 1983), p. 451.  
<sup>7</sup> C. A. Sholl, *J. Phys. C* **14**, 447 (1981).  
<sup>8</sup> R. C. Bowman, Jr., D. R. Torgeson, and A. J. Maeland, *Z. Phys. Chem.* **181**, 725 (1993).  
<sup>9</sup> H. Y. Carr and E. M. Purcell, *Phys. Rev.* **94**, 630 (1954).  
<sup>10</sup> S. Meiboom and D. Gill, *Rev. Sci. Instrum.* **29**, 688 (1958).  
<sup>11</sup> D. R. Torgeson (private communication).  
<sup>12</sup> J. Korrynga, *Physica* **16**, 601 (1950).  
<sup>13</sup> N. Bloembergen, E. M. Purcell, and R. V. Pound, *Phys.*

*Rev.* **73**, 679 (1948).

<sup>14</sup> For simplicity, we ignore a second Lorentzian term with frequency  $2\omega_0$ .  
<sup>15</sup> D. A. Faux, D. K. Ross, and C. A. Sholl, *J. Phys. C* **19**, 4115 (1986); C. A. Sholl, *ibid.* **21**, 319 (1988).  
<sup>16</sup> J. T. Markert, E. J. Cotts, and R. M. Cotts, *Phys. Rev. B* **37**, 6446 (1988).  
<sup>17</sup> C. P. Slichter, *Principles of Magnetic Resonance*, 3rd ed. (Springer, New York, 1990).  
<sup>18</sup> A. Avogadro and M. Villa, *J. Chem. Phys.* **66**, 2359 (1977).  
<sup>19</sup> N. Salibi and R. M. Cotts, *Phys. Rev. B* **27**, 2625 (1983).  
<sup>20</sup> R. L. Kleinberg and B. G. Silbernagel, *Solid State Commun.* **33**, 867 (1980).  
<sup>21</sup> See, for example, P. Freiländer *et al.*, *Z. Phys. Chem. (N.F.)* **151**, 93 (1987), and other articles in that volume.  
<sup>22</sup> P. C. L. Stephenson and C. A. Sholl, *J. Phys. Condens. Matter* **5**, 2809 (1993).  
<sup>23</sup> P. C. L. Stephenson (private communication).